Microchimica Acta (2020) 187: 532
https://doi.org/10.1007/s00604-020-04484-4

ORIGINAL PAPER

Nitrogen-doped graphene quantum dot–based sensing platform for metabolite detection

Xiaotong Liu[1] · Xingguang Su[1]

Received: 6 April 2020 / Accepted: 5 August 2020 / Published online: 31 August 2020

Abstract

A novel fluorescent sensing platform based on nitrogen-doped graphene quantum dots (N-GQDs) is presented, which is able to detect various metabolites (cholesterol, glucose, lactate, and xanthine) rapidly, sensitively, and selectively. Hg^{2+} can attach on the surface of N-GQDs, leading to the quenching of N-GQD fluorescence. In the presence of cysteine (Cys), Hg^{2+} is released from N-GQDs and associates with Cys. Then, the fluorescence of N-GQDs is recovered. Hydrogen peroxide, resulting from the enzymatic oxidation of metabolites, can convert two molecules of Cys into one molecule of cystine, which cannot bind with Hg^{2+}. So, the fluorescence of N-GQDs quenched again. For cholesterol, glucose, lactate, and xanthine, the limits of detection are 0.035 μmol/L, 0.025 μmol/L, 0.07 μmol/L, and 0.04 μmol/L, respectively, and the linear ranges are 1–12 μmol/L, 0.06–3 μmol/L, 0.2–70 μmol/L, and 0.12–17 μmol/L, respectively. The presented method was applied to quantify metabolites in human blood samples with satisfactory results.

Keywords Nitrogen-doped graphene quantum dots · Fluorescent sensing · Metabolites · Cysteine

Introduction

Many metabolic diseases can be monitored by different endogenous metabolites [1]. So, it is of crucial importance to monitor human metabolism for personalized therapy. Therefore, simple and fast protocols for the quantitative detection of metabolites in biological matrices have aroused great interest and are very important for diagnosis and health care [2, 3]. However, current technologies for metabolite assay such as colorimetry [4–6], electrochemistry [7–10], photoelectrochemistry [11], and high-performance liquid chromatography [12–14] often suffer from low selectivity, large sample consumption, complicated pretreatment, bulk instruments, and long waiting time [15]. Each of these makes it infeasible in a typical laboratory and clinic environments. Therefore, there is a need to further develop high sensitivity and selectivity methods for detecting metabolites.

Graphene quantum dots (GQDs) have the advantages of low toxicity, good biocompatibility, high water solubility, chemical inertness, stable photoluminescence, rich surface groups, and easy functionalization [16, 17]. These outstanding properties make them promising candidates for numerous exciting applications, such as medical diagnosis, bioimaging [18, 19], catalysis [20, 21], and photovoltaic devices [22, 23]. The optical and electrical properties of GQDs can be effectively tuned by doping heteroatoms [24, 25]. Having a comparable atomic size and five valence electrons for bonding with carbon atoms, the N atom is popular for chemical doping of carbon nanomaterials [24, 26].

In this work, we developed a novel N-GQD-based label-free biosensor for rapid detection of metabolites (cholesterol, glucose, lactate, and xanthine), which is convenient, sensitive, and low cost. As illustrated in Scheme 1, the positively charged Hg^{2+} may attach on the negatively charged N-GQD surface by electrostatic interaction. This process leads to non-radiative electron/hole recombination and effective electron transfer, which results in the N-GQD fluorescence quenching [27–30]. Based on the previous report, the quenching process was dynamic quenching [31]. In the presence of Cys, Hg^{2+} is released from the surface of N-GQDs and associated with Cys

Electronic supplementary material The online version of this article (https://doi.org/10.1007/s00604-020-04484-4) contains supplementary material, which is available to authorized users.

✉ Xingguang Su
suxg@jlu.edu.cn

[1] Department of Analytical Chemistry, College of Chemistry, Jilin University, Changchun 130012, China

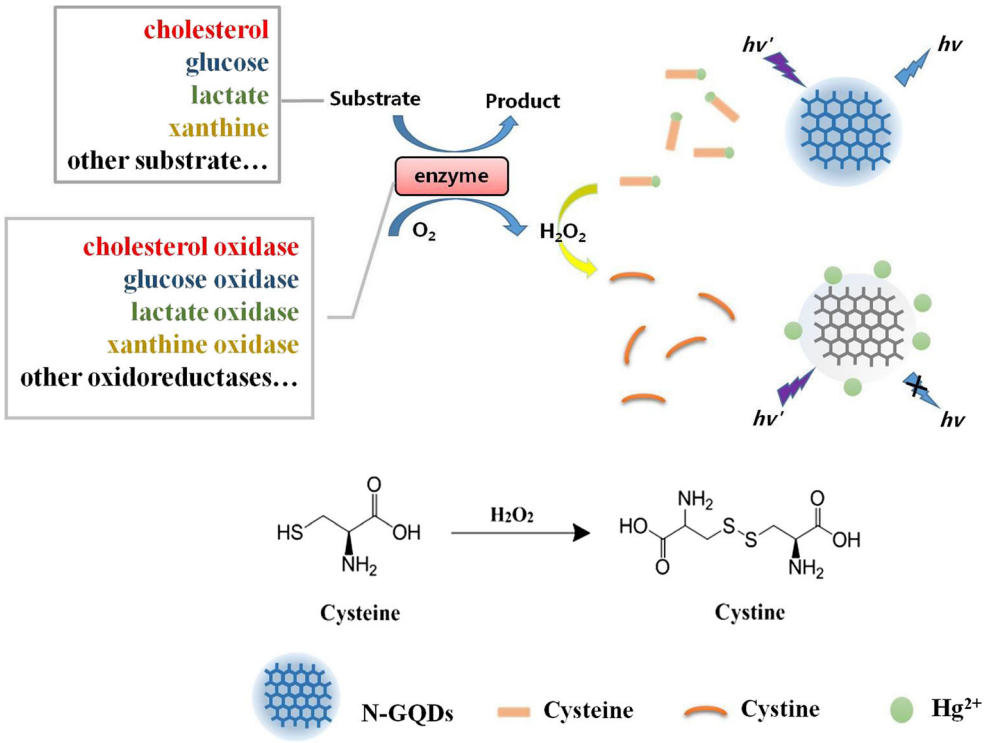

Scheme 1 Schematic illustration of the sensing system based on N-GQDs

via Hg-S bond [28], forming a more stable Hg-Cys complex, which enlarges the distance between Hg^{2+} and N-GQDs, leads to the break of electron transfer, and results in the recovery of N-GQD fluorescence. Hydrogen peroxide, resulting from the enzymatic oxidation of metabolites, such as cholesterol, glucose, lactate, and xanthine, converts two molecules of Cys into one molecule of cystine. This process leads to the conversion of two active thiol groups (-SH) into one inactive disulfide bridge (-SS-) [32], which cannot stably bind with Hg^{2+}. So, the fluorescence of N-GQDs quenched again. Based on the mechanisms illustrated above, a sensitive fluorescence sensing method for metabolite detection is developed.

Experiment

Reagents and chemicals

All chemicals used were at least of analytical reagent grade and used without further purification. The water used in all experiments had a resistivity higher than 18 MΩ/cm. Hydrogen peroxide, NaOH, NaCl, KCl, $CaCl_2$, citric acid, glucose, lactate, and xanthine were obtained from Beijing Dingguo Biotechnology Co., Ltd. Cholesterol, alanine, serine, threonine, aspartic acid, and lysine were obtained from Sigma-Aldrich Chemical Co.

Instruments

The fluorescence spectra were obtained by using a Shimadzu RF-5301 PC fluorophotometer equipped with a xenon lamp using right-angle geometry. UV-vis absorption spectra were obtained by a Varian GBC Cintra 10e UV-vis spectrometer. In both experiments, a 1-cm path-length quartz cuvette was used. FT-IR spectra were recorded by a Bruker IFS66V FT-IR spectrometer equipped with a DGTS detector. Transmission electron microscopy (TEM) was conducted using a Hitachi H-800 electron microscope at an acceleration voltage of 200 kV. XRD patterns were obtained by a Rigaku D/Max 2550 X-ray diffractometer.

Synthesis of N-GQDs

As previously reported [33], N-GQDs were prepared from citric acid (carbon source) and ammonia (nitrogen sources). 2 g citric acid and 0.3 mL ammonia were heated at 210 °C for 6 h together in a Teflon-lined autoclave. 10 mL ultrapure water was used to dissolve the resulting dark brown mixture. Next, the pH of N-GQD dispersion was adjusted to 7.0 by adding NaOH aqueous solution. To remove the large dots, the supernatant was centrifuged at 12,000 rpm for 10 min.

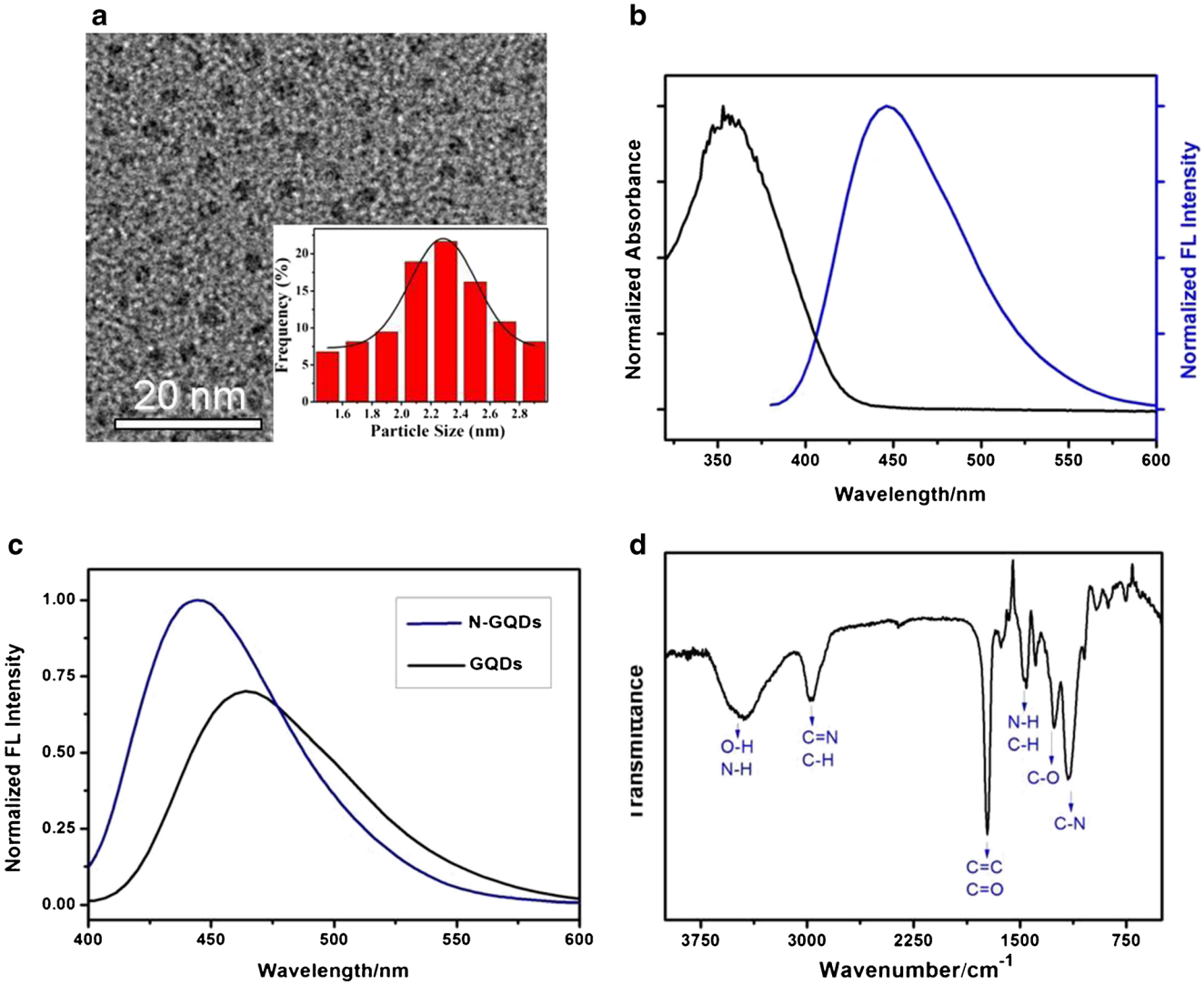

Fig. 1 **a** TEM image of N-GQDs. Inset: size distribution diagram of N-GQDs. **b** Normalized UV-vis absorption spectra and fluorescence emission spectra of N-GQDs. **c** Normalized fluorescence spectra of N-GQDs and undoped GQDs. **d** FT-IR spectra of N-GQDs

Subsequently, the obtained liquid was diluted to 200 mL with ultrapure water. The concentration of as-prepared N-GQD stock solution was 10 mg/mL. Finally, the as-prepared N-GQDs were stored at 4 °C for further use. The quantum yield of N-GQDs is 15.5% by using quinine sulfate as reference.

H_2O_2 detection

For H_2O_2 detection, different amounts of H_2O_2 were added in a series of 1.5 mL solution containing 200 μL N-GQDs, 50 μL PBS (0.2 mol/L, pH = 7.5), 40 μmol/L Hg^{2+}, and 100 μmol/L cysteine. Then, the solution was incubated at 45 °C for 20 min. The fluorescence spectra were recorded in the 400–700-nm wavelength range at the excitation wavelength of 370 nm.

Metabolite detection

For metabolite (cholesterol, glucose, lactate, and xanthine) detection, different amounts of metabolites were added in a series of 1.5 mL solution containing 200 μL N-GQDs, 50 μL PBS (0.2 mol/L, pH = 7.5) and 40 μmol/L Hg^{2+}, 100 μmol/L cysteine, and oxidases (10 μmol/L cholesterol oxidase or 2.5 μmol/L glucose oxidase or 5 μmol/L lactate oxidase or 5 μmol/L xanthine oxidase). The fluorescence spectra were recorded in the 400–700-nm wavelength range at the excitation wavelength of 370 nm.

Real sample assay

The blood samples of healthy persons were supplied by the Hospital of Changchun China, Japan Union Hospital.

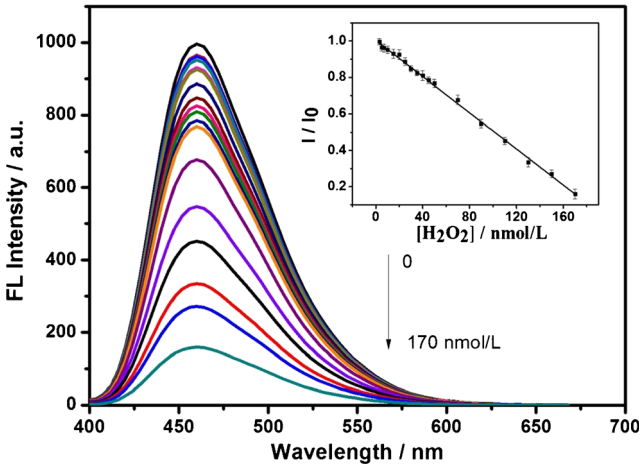

Fig. 2 The fluorescence spectra of N-GQDs/Hg^{2+}/cysteine system with different concentrations of H_2O_2 in the range of 0–170 nmol/L (0, 3, 5, 7, 10, 15, 20, 25, 30, 35, 40, 50, 70, 90, 110, 130, 150, 170 nmol/L) Inset: the relationship between I/I_0 and the concentration of H_2O_2 in the range of 3–170 nmol/L. I and I_0 are fluorescence intensities of the N-GQDs/Hg^{2+}/cysteine system in the presence and absence of H_2O_2 relatively. The error bars were gained from three parallel test results

Acetonitrile was added to the blood samples (the volume of acetonitrile and blood was 1.5:1) and shaken for 2 min. Then, the product was centrifuged at 10000 rpm for 10 min to remove protein. A series of different concentrations of metabolites (cholesterol, glucose, lactate, and xanthine) were added to the obtained serum samples [34]. Then, the samples were subjected to 5-fold dilutions and detected by the method described above. All experiments were performed in compliance with the relevant laws and institutional guidelines, and the writing of informed consent for all samples was obtained from human subjects.

Results and discussion

Characterization and feasibility

The TEM image of N-GQDs is shown in Fig. 1a, which indicates the nearly spherical shape of N-GQDs. The as-prepared N-GQDs are mostly uniform in size and have a diameter of 2.25 nm. The XRD data (Fig. S1) showed that N-GQDs possessed a peak at 22° (002), corresponding to its graphite structure [35, 36]. The UV-vis absorption spectra of N-GQDs (Fig. 1b) show a strong absorbance at 352 nm, which probably result from π-π* transition in aromatic structures [19]. Figure 1a shows the fluorescence spectra of N-GQDs and pure GQDs. It reveals that the fluorescent emission peaks of N-GQDs and GQDs are at 445 nm and 464 nm, respectively. The fluorescent spectra of N-GQDs have a 19-nm blue shift compared with undoped GQDs, which is due to the strong electron affinity of N atoms doped in the N-GQD [37]. In addition, the fluorescence intensity of N-GQDs increased by about 37% than that of GQDs. The N-doping-induced modulation of the electronic and chemical characteristics of the N-GQDs may contribute to the highly efficient fluorescent emission [38]. The FT-IR spectra were used to study the existence of surface functional groups of N-GQDs. As shown in Fig. 1d, the FT-IR spectrum of N-GQDs reveals the C-N stretching vibrations at 1159 cm^{-1} and the C-O bending vibrations at 1261 cm^{-1}, N-H and C-H bending vibrations at 1450 cm^{-1}, C=C and C=O stretching vibrations at 1720 cm^{-1}, C=N and C-H stretching vibrations at 2966 cm^{-1}, and absorption bands of O-H and N-H stretching vibrations at 3437 cm^{-1}, which indicated the presence of carboxyl and hydroxyl functional groups on the surface of N-GQDs.

The feasibility study of the proposed method was conducted. As shown in Fig. S2 (A), Besides Hg^{2+}, other metal ions such as Ag^{+} and Cu^{2+} can also quench the fluorescence of N-GQDs, but the binding strength between these ions and N-GQDs is much weaker than Hg^{2+}. As reported in the literature, it is probably because the Hg^{2+} ions have a stronger affinity towards the carboxylic groups on the GQDs surface than other metal ions [27, 39, 40]. Thus, their quenching ability is not as strong as Hg^{2+}. The relationship between I/I_0 and the concentration of Hg^{2+} in the range of 0–70 μmol/L is shown in Fig. S2(B). I and I_0 are fluorescence intensities of the N-GQDs in the presence and absence of Hg^{2+} relatively. Figure S3(A) shows that there is no significant change in the fluorescence intensity of N-GQDs after mixing with H_2O_2 or Cys. A significant decrease in fluorescence intensity can be observed after mixing with Hg^{2+}. After adding cysteine to N-GQDs/Hg^{2+} system, the fluorescence intensity recovered to about 91% of the original N-GQDs. However, after adding H_2O_2, the fluorescence intensity decreased again. The inset of Fig. S3(A) shows the photo of a probe system solution before and after H_2O_2 addition under a UV lamp. According to Fig. S3(B, C), metabolites or metabolite oxidases cannot influence the fluorescence intensity of N-GQDs, N-GQDs/Hg^{2+}, or N-GQDs/Hg^{2+} system, which indicates they are not able to bind to Hg^{2+} or N-GQDs.

Optimization for detection conditions

In order to optimize the conditions for H_2O_2 detection, we investigated the effects of incubation time, pH, and temperature on the fluorescence intensity of N-GQDs/Hg^{2+}/cysteine/H_2O_2 system. As shown in Fig. S4, the fluorescence intensity of N-GQDs (A) decreased within 15 min; (B) decreased with the increase of pH value until 7.5; and (C) decreased with the increase of temperature between 25 and 45 °C. Thus, we adopted 20 min as the reaction time, 45 °C as an optimized temperature, and chose PBS buffer solution (pH = 7.5).

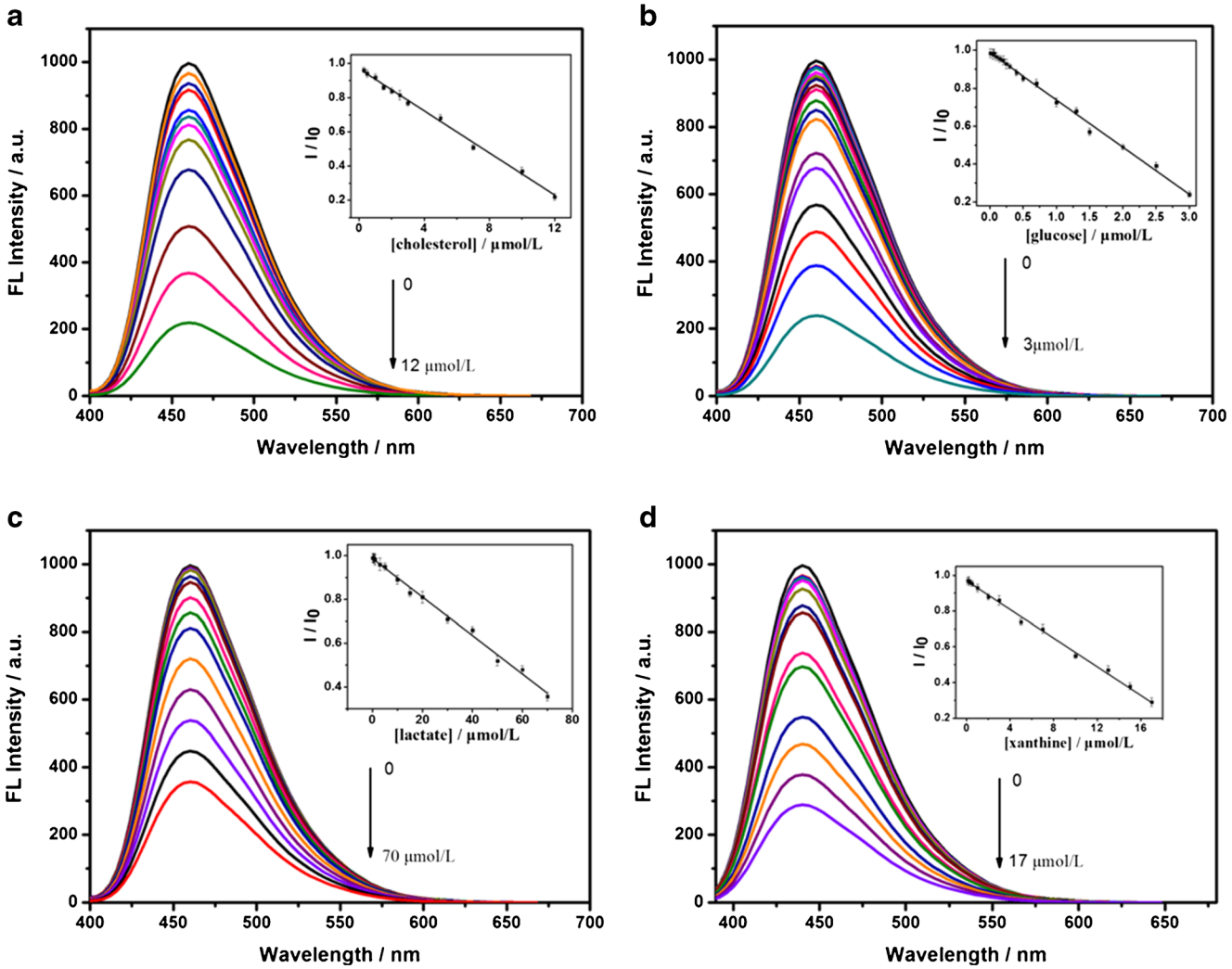

Fig. 3 The fluorescence spectra of N-GQDs/Hg^{2+}/cysteine system with different concentrations of **a** cholesterol (0, 1, 1.5, 2, 2.5, 3, 5, 7, 10, 12 μmol/L); inset: the relationship between I/I_0 and the concentration of cholesterol in the range of 1–12 μmol/L; **b** glucose (0, 0.06, 0.01, 0.05, 0.1, 0.2, 0.25, 0.3, 0.4, 0.5, 0.7, 1, 1.3, 1.5, 2, 2.5, 3 μmol/L); inset: the relationship between I/I_0 and the concentration of glucose in the range of 0.06–3 μmol/L; **c** lactate (0, 0.2, 1, 3, 5, 10, 15, 20, 30, 40, 50, 60, 70 μmol/L); inset: the relationship between I/I_0 and the concentration of lactate in the range of 0.2–70 μmol/L; **d** xanthine (0, 0.12, 0.2, 0.3, 0.5, 1, 2, 3, 5, 7, 10, 13, 15, 17 μmol/L); inset: the relationship between I/I_0 and the concentration of xanthine in the range of 0.12–17 μmol/L. I and I_0 are fluorescence emission intensities of the detection system in the presence and absence of metabolites relatively. The error bars were obtained from three parallel test results

As for the detection of metabolites (cholesterol, glucose, lactate, and xanthine), the effect of oxidase concentrations, reaction temperatures, pH, and incubation times on the detection of metabolites were studied (Fig. S5), and the optimal detection conditions are listed in Table S1.

Detection for H_2O_2

Under the optimal conditions, the fluorescence spectra of N-GQDs/Hg^{2+}/cysteine system with various concentrations of H_2O_2 are shown in Fig. 2. It can be seen that the fluorescence intensity of the system decreases rapidly with the increase of

Table 1 The linear regression equations, linear ranges, R^2, and LOD of metabolites

Analyte	Regression equation	Linear range (μmol/L)	R^2	LOD (μmol/L)
Cholesterol	$I/I_0 = 0.969–0.0612$[cholesterol] (μmol/L)	1–12	0.995	0.035
Glucose	$I/I_0 = 0.989–0.249$ [glucose] (μmol/L)	0.06–3	0.998	0.025
Lactate	$I/I_0 = 0.988–0.009$[lactate] (μmol/L)	0.2–70	0.996	0.07
Xanthine	$I/I_0 = 0.970–0.039$[xanthine] (μmol/L)	0.12–17	0.997	0.04

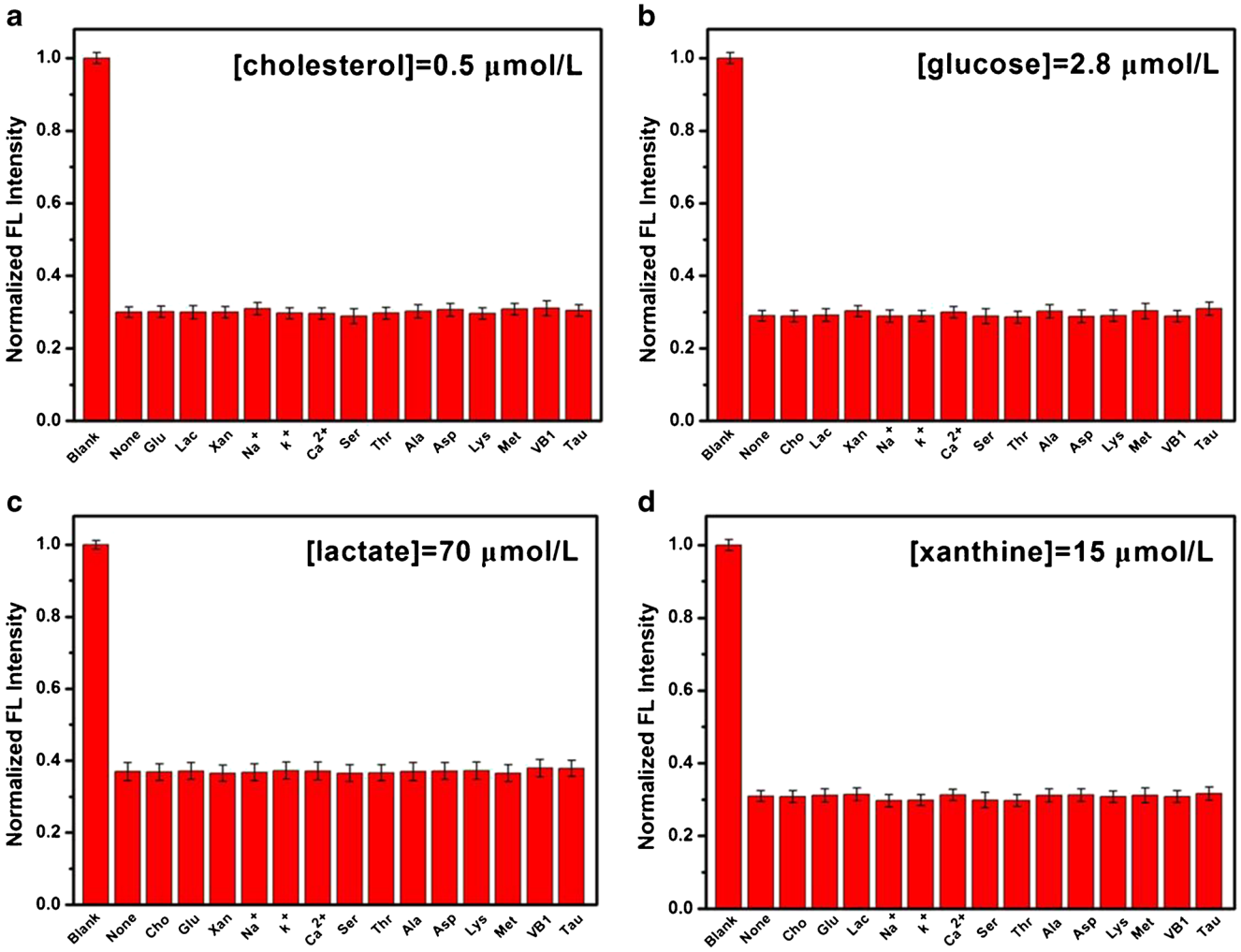

Fig. 4 The interference of potentially interfering substances (Na^+ (2000 μmol/L), K^+ (2000 μmol/L), Ca^{2+} (2000 μmol/L), Ser (1000 μg/L), Thr (1000 μg/L), Ala (1000 μg/L), Met (1000 μg/L), VB1 (1000 μg/L), Tau (1000 μg/L), and Lys (1000 μg/L)) on the determination for **a** cholesterol (0.5 μmol/L), **b** glucose (2.8 μmol/L), **c** lactate (70 μmol/L), and **d** xanthine (15 μmol/L). As potential interfering substances, the concentrations of cholesterol, glucose, lactate, and xanthine are 5 μmol/L, 20 μmol/L, 300 μmol/L and 100 μmol/L, respectively

H_2O_2 concentration. The relative fluorescence intensity I/I_0 of N-GQDs/Hg^{2+}/cysteine/H_2O_2 system has a linear correlation with H_2O_2 concentration in the range of 3–170 nmol/L (Fig. 2, inset). The linear regression equation is

$$I/I0 = 1.004 - 0.005[H2O2]\ (\text{nmol/L})$$

The coefficient of determination is $R^2 = 0.996$. The limit of detection (LOD) for H_2O_2 was 1.02 nmol/L. The LOD was based on the equation LOD = $3\sigma/s$, where σ was the standard deviation of the blank signals of the N-GQDs/Hg^{2+}/cysteine system and s was the slope of the calibration curve.

A comparison of linear ranges and LOD between this work and that of other detection methods is listed in Table S2. Compared with other work, our method offers a satisfactory linear range and LOD.

Detection for metabolites

Under the optimal conditions, the fluorescence spectra of N-GQDs/Hg^{2+}/ cysteine system with various concentrations of metabolites (cholesterol, glucose, lactate, and xanthine) are shown in Fig. 3. It can be seen that the fluorescence intensities of the detection system were all significantly decreased with the increasing concentration of metabolites. For cholesterol, glucose, lactate, and xanthine, the linear ranges are 1–12 μmol/L, 0.06–3 μmol/L, 0.2–70 μmol/L, and 0.12–17 μmol/L, respectively. And the limits of detection are 0.035 μmol/L, 0.025 μmol/L, 0.07 μmol/L, and 0.04 μmol/L, respectively. The linear regression equations, linear ranges, R^2, and LOD are shown in Table 1. The

concentrations of cholesterol, glucose, lactate, and xanthine in healthy human adult blood are supposed to be between 2.9 and 6.0 mmol/L; 3.9 and 7.8 mmol/L; 0 mmol/L; and 155 and 428 μmol/L, respectively [34]. So, the proposed method has sufficient sensitivity for the determination of these metabolites in real serum samples. A comparison of linear ranges and LOD between this work with that of other detection methods is listed in Tables S3–S6. Compared with other works, our method offers relatively good linear ranges and LOD.

Interference study

As shown in Fig. 4, the selectivity of the present fluorescence method was testified by investigating the fluorescence response of the sensing system to other potential interfering substances including Na^+, K^+, Ca^{2+}, serine (Ser), threonine (Thr), alanine (Ala), lysine (Lys), methionine (Met), vitamin B_1 (VB1), and taurine (Tau). As potential interfering substances in the detection for other metabolites, the effects of cholesterol, glucose, lactate, and xanthine are also studied. The "Blank" column indicates there is no analyte or interference, the "None" column indicates there is only analyte but no interference in the detection system, and others show the coexisting of analyte with one of the interferences. The results indicated that this detection method has satisfactory selectivity against common metal ions and biomolecules. As shown in Fig. 4, with the other metabolites present, the system exhibited an identical response to the selected analytes, revealing this method can distinguish the selected analytes if many of them are present concurrently owing to the specific catalyzation of different oxidases to its substrate.

Real sample detection

To further demonstrate the practicality of the proposed detection method, we detected the concentration of cholesterol, glucose, lactate, and xanthine in human blood by standard addition method, and the results are listed in Table S7. It shows that the recoveries of these four metabolites are in the range of 98.2–101.8%. The relative standard deviations (RSD) were no more than 2.1%. These results demonstrated that the method developed in this work has potential applications in the practical measurement of metabolites. Nevertheless, this fluorescence assay also has its limitations, such as the potential toxicity of Hg^{2+} may hinder the utilization in intracellular sensing, and working under the ultraviolet excitation leads to prone interferences by biological substrates. Thus, the construction of fluorescent probes with superior biocompatibility and anti-interference ability is still needed in the following work.

Conclusion

In this work, a facile fluorescence sensing platform has been developed based on N-GQDs. It enables rapid, ultrasensitive, and selective detection of metabolites in human blood sample. This method has the potential in the diagnosis of metabolic disorders and other associated diseases. Combined with smart-phone-based or other portable fluorometers, the detection method developed in this work is also available for home-based healthcare.

Funding This work is supported by the National Natural Science Foundation of China (No. 21775052 and No. 21575048) and the Science and Technology Development Project of Jilin province, China (No. 20180414013GH).

Compliance with ethical standards

All experiments were performed in compliance with the relevant laws and institutional guidelines, and the writing of informed consent for all samples was obtained from human subjects.

Conflict of interest The authors declare that they have no competing interests.

References

1. Ghoreishizadeh SS, Carrara S, Micheli GD (2011) Circuit design for human metabolites biochip. In: 2011 IEEE Biomedical Circuits and Systems Conference (BioCAS): 10–12 Nov. 2011. 460–463
2. Vaidyanathan S, Goodacre R (2007) Quantitative detection of metabolites using matrix-assisted laser desorption/ionization mass spectrometry with 9-aminoacridine as the matrix. Rapid Commun Mass Spectrom 21(13):2072–2078
3. Ma Z, Wu T, Li P, Liu M, Huang S, Li H, Zhang Y, Yao S (2019) A dual (colorimetric and fluorometric) detection scheme for glutathione and silver (I) based on the oxidase mimicking activity of MnO2 nanosheets. Microchim Acta 186(8):498
4. Cai X, Gao X, Wang L, Wu Q, Lin X (2013) A layer-by-layer assembled and carbon nanotubes/gold nanoparticles-based bienzyme biosensor for cholesterol detection. Sensors Actuators B Chem 181:575–583
5. Nantaphol S, Chailapakul O, Siangproh W (2015) Sensitive and selective electrochemical sensor using silver nanoparticles modified glassy carbon electrode for determination of cholesterol in bovine serum. Sensors Actuators B Chem 207:193–198
6. Pu W, Zhao H, Wu L, Zhao X (2015) A colorimetric method for the determination of xanthine based on the aggregation of gold nanoparticles. Microchim Acta 182(1–2):395–400
7. Umar A, Ahmad R, Hwang SW, Kim SH, Al-Hajry A, Hahn YB (2014) Development of highly sensitive and selective cholesterol biosensor based on cholesterol oxidase co-immobilized with α-Fe2O3 micro-pine shaped hierarchical structures. Electrochim Acta 135:396–403
8. Amiri-Aref M, Raoof JB, Ojani R (2014) A highly sensitive electrochemical sensor for simultaneous voltammetric determination of noradrenaline, acetaminophen, xanthine and caffeine based on a flavonoid nanostructured modified glassy carbon electrode. Sensors Actuators B Chem 192:634–641

9. Rassas I, Braiek M, Bonhomme A, Bessueille F, Raffin G, Majdoub H, Jaffrezic-Renault N (2019) Highly sensitive voltammetric glucose biosensor based on glucose oxidase encapsulated in a chitosan/kappa-carrageenan/gold nanoparticle bionanocomposite. Sensors 19(1)
10. Ricardo Romero M, Ahumada F, Garay F, Baruzzi AM (2010) Amperometric biosensor for direct blood lactate detection. Anal Chem 82(13):5568–5572
11. Atchudan R, Muthuchamy N, Edison TNJI, Perumal S, Vinodh R, Park KH, Lee YR (2019) An ultrasensitive photoelectrochemical biosensor for glucose based on bio-derived nitrogen-doped carbon sheets wrapped titanium dioxide nanoparticles. Biosens Bioelectron 126:160–169
12. Parpinello GP, Versari A (2000) A simple high-performance liquid chromatography method for the analysis of glucose, glycerol, and methanol in a bioprocess. J Chromatogr Sci 38(6):259–261
13. Daneshfar A, Khezeli T, Lotfi HJ (2009) Determination of cholesterol in food samples using dispersive liquid-liquid microextraction followed by HPLC-UV. J Chromatogr B Anal Technol Biomed Life Sci 877(4):456–460
14. Biagi S, Ghimenti S, Onor M, Bramanti E (2012) Simultaneous determination of lactate and pyruvate in human sweat using reversed-phase high-performance liquid chromatography: a noninvasive approach. Biomed Chromatogr 26(11):1408–1415
15. Qiu Y, Cai G, Su M, Chen T, Zheng X, Xu Y, Ni Y, Zhao A, Xu LX, Cai S, Jia W (2009) Serum metabolite profiling of human colorectal cancer using GC-TOFMS and UPLC-QTOFMS. J Proteome Res 8(10):4844–4850
16. Zhu SJ, Meng QN, Wang L, Zhang JH, Song YB, Jin H, Zhang K, Sun HC, Wang HY, Yang B (2013) Highly photoluminescent carbon dots for multicolor patterning, sensors, and bioimaging. Angew Chem Int Ed 52(14):3953–3957
17. Liu J, Chen Y, Wang W, Feng J, Liang M, Ma S, Chen X (2016) "Switch-on" fluorescent sensing of ascorbic acid in food samples based on carbon quantum dots-MnO2 probe. J Agric Food Chem 64(1):371–380
18. Zhu S, Zhang J, Liu X, Li B, Wang X, Tang S, Meng Q, Li Y, Shi C, Hu R, Yang B (2012) Graphene quantum dots with controllable surface oxidation, tunable fluorescence and up-conversion emission. RSC Adv 2(7):2717–2720
19. Fang Y, Guo S, Li D, Zhu C, Ren W, Dong S, Wang E (2012) Easy synthesis and imaging applications of cross-linked green fluorescent hollow carbon nanoparticles. ACS Nano 6(1):400–409
20. Li HT, He XD, Kang ZH, Huang H, Liu Y, Liu JL, Lian SY, Tsang CHA, Yang XB, Lee ST (2010) Water-soluble fluorescent carbon quantum dots and photocatalyst design. Angew Chem Int Ed 49(26):4430–4434
21. Zhuo S, Shao M, Lee S-T (2012) Upconversion and downconversion fluorescent graphene quantum dots: ultrasonic preparation and photocatalysis. ACS Nano 6(2):1059–1064
22. Gupta V, Chaudhary N, Srivastava R, Sharma GD, Bhardwaj R, Chand S (2011) Luminscent graphene quantum dots for organic photovoltaic devices. J Am Chem Soc 133(26):9960–9963
23. Feng X, Marcon V, Pisula W, Hansen MR, Kirkpatrick J, Grozema F, Andrienko D, Kremer K, Müllen K (2009) Towards high charge-carrier mobilities by rational design of the shape and periphery of discotics. Nat Mater 8(5):421–426
24. Li Y, Zhao Y, Cheng H, Hu Y, Shi G, Dai L, Qu L (2012) Nitrogen-doped graphene quantum dots with oxygen-rich functional groups. J Am Chem Soc 134(1):15–18
25. Moniruzzaman M, Kim J (2019) N-doped carbon dots with tunable emission for multifaceted application: solvatochromism, moisture sensing, pH sensing, and solid state multicolor lighting. Sensors Actuators B Chem 295:12–21
26. Ganganboina AB, Dutta Chowdhury A, Doong R (2017) N-doped graphene quantum dots decorated V2O5 nanosheet for fluorescence turn off-on detection of cysteine. ACS Appl Mater Interfaces: acsami.7b15120
27. Wu Z, Li W, Chen J, Yu C (2014) A graphene quantum dot-based method for the highly sensitive and selective fluorescence turn on detection of biothiols. Talanta 119:538–543
28. Zhou L, Lin Y, Huang Z, Ren J, Qu X (2012) Carbon nanodots as fluorescence probes for rapid, sensitive, and label-free detection of Hg2+ and biothiols in complex matrices. Chem Commun 48(8): 1147–1149
29. Li L, Wang C, Liu K, Wang Y, Liu K, Lin Y (2015) Hexagonal cobalt oxyhydroxide–carbon dots hybridized surface: high sensitive fluorescence turn-on probe for monitoring of ascorbic acid in rat brain following brain ischemia. 87(6):3404–3411
30. Ma Z, Sun Y, Xie J, Li P, Lu Q, Liu M, Yin P, Li H, Zhang Y, Yao S (2020) Facile preparation of MnO2 quantum dots with enhanced fluorescence via microenvironment engineering with the assistance of some reductive biomolecules. ACS Appl Mater Interfaces 12(13):15919–15927
31. Shi B, Zhang L, Lan C, Zhao J, Su Y, Zhao S (2015) One-pot green synthesis of oxygen-rich nitrogen-doped graphene quantum dots and their potential application in pH-sensitive photoluminescence and detection of mercury (II) ions. Talanta 142:131–139
32. Barroso J, Diez-Buitrago B, Saa L, Moller M, Briz N, Pavlov V (2018) Specific bioanalytical optical and photoelectrochemical assays for detection of methanol in alcoholic beverages. Biosens Bioelectron 101:116–122
33. Chen S, Chen X, Xia T, Ma Q (2016) A novel electrochemiluminescence sensor for the detection of nitroaniline based on the nitrogen-doped graphene quantum dots. Biosens Bioelectron 85:903–908
34. Ian BW (2017) Oxford handbook of clinical medicine, Tenth edn. GB, Oup Oxford
35. Liu Y, Tang X, Deng M, Cao Y, Li Y, Zheng H, Li F, Yan F, Lan T, Shi L, Gao L, Huang L, Zhu T, Lin H, Bai Y, Qu D, Huang X, Qiu F (2019) Nitrogen doped graphene quantum dots as a fluorescent probe for mercury (II) ions. Microchim Acta 186(3):140
36. Zhang M, Bai L, Shang W, Xie W, Ma H, Fu Y, Fang D, Sun H, Fan L, Han M, Liu C, Yang S (2012) Facile synthesis of water-soluble, highly fluorescent graphene quantum dots as a robust biological label for stem cells. J Mater Chem 22(15):7461–7467
37. Liu S, Tian J, Wang L, Zhang Y, Qin X, Luo Y, Asiri AM, Al-Youbi AO, Sun X (2012) Hydrothermal treatment of grass: a low-cost, green route to nitrogen-doped, carbon-rich, photoluminescent polymer nanodots as an effective fluorescent sensing platform for label-free detection of Cu (II) ions. Adv Mater 24(15):2037–2041
38. Ju J, Chen W (2014) Synthesis of highly fluorescent nitrogen-doped graphene quantum dots for sensitive, label-free detection of Fe (III) in aqueous media. Biosens Bioelectron 58:219–225
39. Li Z, Wang Y, Ni Y, Kokot S (2015) A rapid and label-free dual detection of Hg (II) and cysteine with the use of fluorescence switching of graphene quantum dots. Sensors Actuators B Chem 207:490–497
40. Chai F, Wang T, Li L, Liu H, Zhang L, Su Z, Wang C (2010) Fluorescent gold nanoprobes for the sensitive and selective detection for Hg2+. Nanoscale Res Lett 5(11):1856–1860